JOURNAL OF AGRICULTURE AND APPLIED BIOLOGY
2024, Vol. 5, No. 2, 178 - 193
http://dx.doi.org/10.11594/jaab.05.02.04
E-ISSN: 2723-5106

Research Article

Using USLE, GIS and remote sensing for the soil loss assessment in the National Park of Theniet El Had, Algeria

Sahnoun Fellah[1,2]*, Benali Benzater[2]*, Laïd Guemou[1], Anouar Hachemaoui[2], Mohamed Nadjib Benzohra[1], Abdelkader Elouissi[2], Abderrahmane Hamimed[2]

[1]Nature and Life Sciences Department, Faculty of Sciences and Technology, University of Tissemsilt, Algeria
[2]Biological Systems and Geomatics Research Laboratory (LRSBG), Mustapha Stambouli University of Mascara, 29000, Mascara, Algeria

Article history:

Submitted 05 May 2024
Accepted 07 June 2024
Revised 09 July 2024
Published 27 August 2024

Keywords:

Cartography
GIS
Remote Sensing
THNP (Algeria)
USLE
Water erosion

***Corresponding author:**

E-mail:

fellah.sahnoun@univ-tissemsilt.dz
benzaterbenali@gmail.com

Abstract

Soil water erosion is one of the problems that affect the environment, agriculture and social life by threatening several land surfaces. The objective of this study is to use the USLE model, GIS and remote sensing (RS) to estimate the annual rate of soil loss by water erosion in the Theniet El Had National Park (THNP) which belongs to the mountainous ecosystem of Djebel El Meddad, located in the northwest of Algeria. The use of the USLE model takes into account the five factors controlling water erosion, namely: the rain erosivity (R) determined from the annual rainfall data, the soil erodibility (K) developed from soil survey data, the slope lengths (LS) generated by using DEM, the vegetation cover (C) by the use of RS data and erosion control management practices (P) by field trips. The integration of these factors made it possible to establish the quantitative map of the annual rate of soil loss varying between 0.02 and 55.10 (t/ha.year), with an average of around 6.64 (t/ha.year). Five erosion aggressiveness classes are used; very weak, weak, moderate, strong and very strong which represent a rate respectively of 23.70, 44.65, 22.72, 4.41 and 4.52 % of the study area surface. The areas with high and very high erosion rates are located in the north having a very rugged relief and low vegetation cover. This study can be used in the mountainous ecosystems and it will make it possible to set up priority intervention zones to combat the risk of water erosion.

How to cite:
Fellah, S., Benzater, B, Guemou, L., Hachemaoui, A., Benzohra, M. N., Elouissi, A., & Hamimed, A. (2024). Using USLE, GIS and remote sensing for the soil loss assessment in the National Park of Theniet El Had, Algeria. *Journal of Agriculture and Applied Biology, 5*(2): 178 - 193. doi: 10.11594/jaab.05.02.04

1. Introduction

Soil is an irreplaceable edaphic factor essential for agriculture. A reduction or persistent loss of soil productivity, through water erosion for example, can lead to desertification and land abandonment (Ferreira et al., 2022). Water erosion is a natural process that, over geological ages, continuously shapes the earth's surface (Markose & Jayappa, 2016). This phenomenon presents the most developed form of physical soil degradation that affects landforms (Nagdeve et al., 2021). It results from the impact of the combination of several natural factors, represented by the aggressiveness of the showers after a long period of drought, the soil lithology fragility, the relief with steep slopes, as well as the vegetation cover (Bouguerra et al., 2017), and amplified by anthropogenic activities such as irrational logging (Hachemaoui et al., 2022), inappropriate agricultural practices and overgrazing (Bouhadeb et al., 2018). Water erosion is a process starting with the detachment of particles under the rain splash impact (Benzater et al., 2019), then its transport by surface runoff and finally deposition of soil particles (Toumi et al., 2013).

Water erosion has considerable impacts on society, the agricultural, economic, environmental sector and water reserves (Yesuph & Dagnew, 2019), the most significant consequences of which are deforestation and drop productivity of arable agricultural land (Girmay et al., 2020; Kolli et al., 2021; Medjani et al., 2023), it reduces soil fertility by depleting nutrients (Panagos et al., 2018), Water runoff from eroded soils degrades the ecological environment by contributing to pollution and altering the quality of water sources (Hategekimana et al., 2020), silting up watercourses and aggravating flooding (Xu et al., 2019), causing a reduction in the storage capacity of dam reservoirs (Meddi et al., 2016) and drinking water (Panagos et al., 2024), and increasing rural exodus (Benchetrit, 1972).

In recent decades, and with the aim of quantifying water erosion, several methods have been developed, associated with geomatics tools ("GIS" and "RS") (Khaoula & Sihem, 2021), offering the possibility of monitoring the spatio-temporal evolution of this phenomenon (Sahnoun et al., 2021; Vrieling, 2006). Among these methods developed by researchers, some are physically based and others are empirical such as the USLE model by Wischmeier and Smith (1978), the MUSLE and the RUSLE (Djoukbala et al., 2019), characterized by the accessibility of the data, its precision, its simplicity and its robustness for the spatialization of water erosion (Bensekhria & Bouhata, 2022). The combination of the USLE model and spatialization techniques which are quantitative tools that can process and analyze the main factors acting on erosion (Koussa & Bouziane, 2019). These factors represent soil erodibility, land exposure and slope length, rainfall erosivity, agricultural practices, and vegetation cover. (Sheikh et al., 2011), to map the average annual soil loss (Toumi et al., 2013). The Mediterranean region is recognized as being susceptible to land degradation and at significant risk of desertification (Ferreira et al., 2022) It is frequent: in Algeria (Saoud & Meddi, 2022; Mahleb et al., 2022); in Tunisia (Sonia et al., 2022); in Morocco (Bou-Imajjane & Belfoul, 2020); in Lebanon (Hassan et al., 2018) in Italy (Rellini et al., 2019) and in Spain (Milazzo et al., 2022). Mountainous areas are considerably vulnerable to water erosion due to their steep slopes, land use land cover (LULC) change and sensitive to climate change (Mandal et al., 2023; Belay et al., 2022).

The objective of this study is to estimate the annual soil loss rate by water erosion and to map its spatial distribution in the very vulnerable mountainous ecosystem of Djebel El Meddad located in THNP (northwest of Algeria) using Wischmeier's empirical USLE model combined with GIS and RS techniques.

2. Materials and methods

2.1 Study area

The study area is THNP presenting a mountainous ecosystem. It is a protected natural area since 1923 following its classification as a diversified ecological site (Mairif et al., 2023). The park is located in Tissemsilet in the northwest of Algeria between latitude 35°51'56'' N and 35°53'04' N, longitudes 01°55'30'' E and 02°01'30'' E, 185 km from the capital Algiers, and 150 km from the Mediterranean coast, covering an area of 3424 ha with an altitude ranging from 858 m to 1787 m (Figure 1),

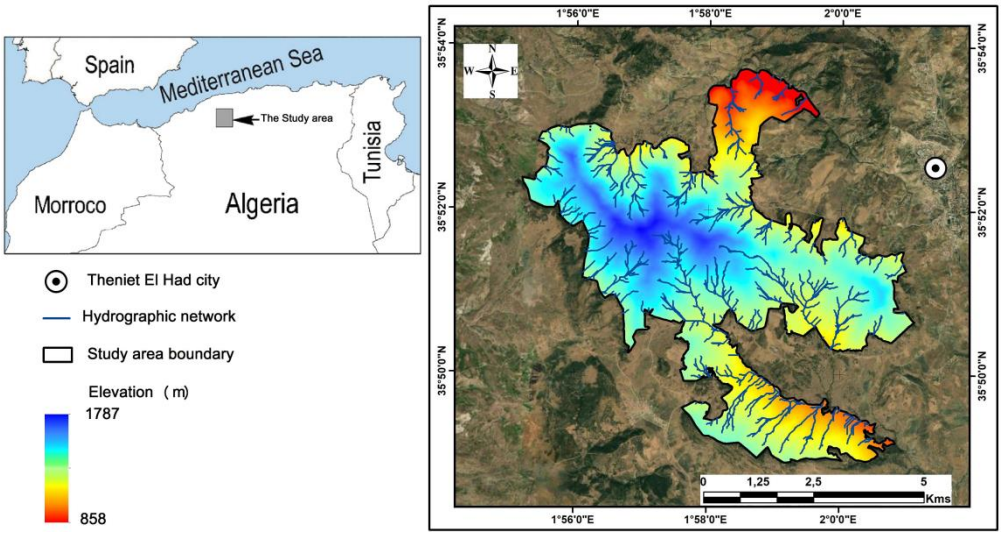

Figure 1. Location of THNP

The THNP is characterized by rugged mountainous relief very sensitive to water erosion; it occupies the two main slopes of Djebel El Meddad (Lamine et al., 2016). The southern slope has more or less steep slopes of 25° maximum. On the other hand, the steep slopes estimated on average at 40° inclination are on the northern slope (Sarmoum et al., 2018). The soils of the study site are deep to superficial in places, poor in organic matter, with a clayey-sandy texture, found on both slopes of the park. They are formed as a result of deposits of particles from eroded slopes. The THNP is subject to the bioclimatic stage characterized by two major periods, the first cold during the winter months with minimum temperatures reaching -1°C and an average annual rainfall varying between 733 mm and 984 mm (Sarmoum et al., 2018), the snowfall in the park is very intense and frosts are very frequent during this period, the second is a dry period during the summer months with a maximum temperature of 30°C. The land use of the THNP consists mainly of cedar which occupies 3/5 of the forest stands on the southern slope, the warmest, on the other hand the northern slope which is the coldest and wetter, the Cedrus atlantica covers 2/3 of the area of this forest massif (Mairif et al., 2023).

2.2 Methods

In this paper, the USLE model of Wischmeier and Smith (1978) was applied to evaluate soil loss (A) in (t/ha.year). This method is a function of five factors in raster format affecting the rate of erosion, namely: rainfall, soil erodibility, slopes, the erosion control management practices and land use. These factors fluctuate spatiotemporally and are influenced by other input data. The USLE model is presented in (Eq. 1):

$$A = R \times K \times LS \times C \times P \quad (1)$$

Where A is the possible average annual soil losses (t/ha.year), R is the erosivity factor of the precipitation characterizing the climatic aggressiveness (MJ.mm/ha.h.year), K is the factor of soil erodibility (t.h/MJ.mm), LS is the factor which presents the length-slope (dimensionless), C is the coverage factor (dimensionless) and P is the erosion control practices factor (dimensionless). In the present study, the spatial distribution of soil loss was obtained by combining the USLE model, GIS and RS techniques; the flowchart (Figure 2) illustrates the methodology adopted and the different data used to calculate the five soil erosion factors presented in (Table 1), the results are generated in the form of thematic maps and tables.

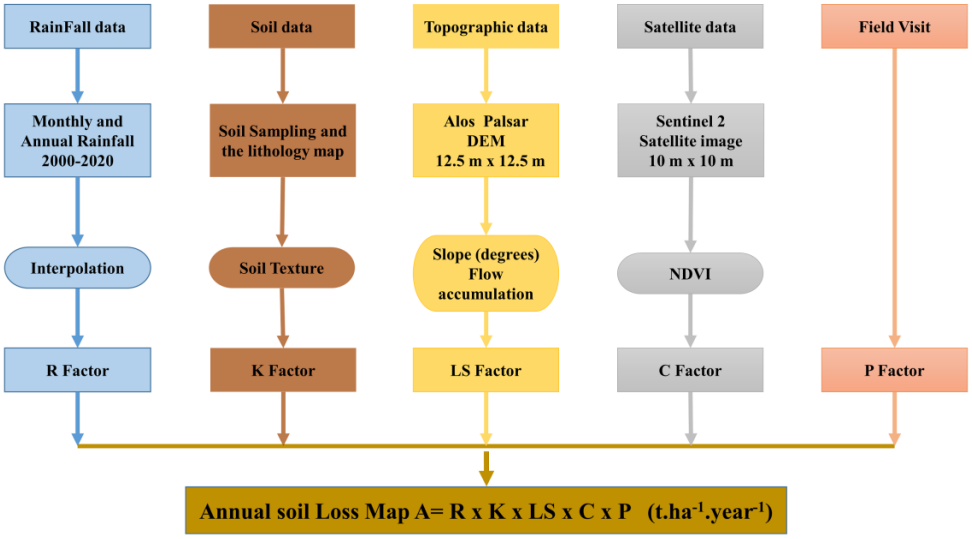

Figure 2. Methodological flowchart of the applied USLE equation

Table1. The data used by the USLE model to map soil erosion

Data type	Description	Data Format	Data source	USLE Factor
Monthly and Annual rainfall	Annual rainfall collected by 10 precipitation station	Excel	National weather center	R factor
Soil data	Soil sampling and the lithology map	Vector (Shape)	15 soil samples distributed over the study site and the lithology map from THNP	K factor
Alos Palsar DEM	Resolution: 12.5 m	Raster	The Alaska Satellite Facility https://asf.alaska.edu/	LS factor
Sentinel 2 satellite image	Acquisition Date: 04-01-2023	Raster	European Space Agency (ESA) for Earth observation https://scihub.copernicus.eu/	C factor

2.2.1. The R factor

Rain is a key driver of soil erosion, which occurs in the absence or reduction of rainwater infiltration, amplifying the driving forces that uproot and carry away soil particles. The factor R (MJ.mm/ha.h.year) expresses the capacity of the rains to erode, the more intense and long-lasting they are, the more they erode the soil. Wischmeier and Smith (1978) proposed the equation to

calculate both the kinetic energy (Ec) and the mean precipitation intensity in 30 mm for a given period and in a well-defined site. Due to data limitations, these hourly data are rarely available at rainfall stations located in this region, so it is difficult to apply this equation to calculate the R factor. To circumvent this constraint, the equation (Eq. 2) proposed by Rango and Arnoldus (1987) is used which allows the calculation of R according to the monthly and annual average precipitation data of 10 rainfall stations bordering our study site spread over a period of 20 years.

$$LogR = 1.74 \times log \sum \left(\frac{P_i^2}{P} \right) + 1.29 \quad (2)$$

Where R is rainfall erosivity (MJ.mm/ha.h.year), Pi is the monthly precipitation (mm), and P is the annual precipitation (mm). Then, the specific results of the rainfall erosivity index R, calculated for each station, were spatialized by interpolation.

2.2.2. The K factor

The soil erodibility factor K (t.h/MJ.mm) expresses the ease with which soil particles are eroded by rain. This factor depends on the texture, soil organic matter content and soil permeability. These properties are not available for the study site. The equation (Eq. 3) established by Wischmeier and Smith (1978) could not be used in this study.

$$K = 2.1 \times M^{1.14} \times 10^{-6} (12 - a) + 0.0325 \times (b - 2) + 0.025 \times (c - 3) \quad (3)$$

Where K is the soil erodibility factor (t.h/MJ.mm), M the particle-size parameter, and is calculated by the formula M= (% of very fine sand+ % of silt x (100% clay)), a is the Organic matter content (% C x 1.724) and b is the soil structure and c is soil permeability. The soil data used for the spatialization of the K factor were extracted from the lithology map established by the THNP and using the Particle size analyzes carried out on 15 soil samples distributed over the study site. The soil textures obtained were categorized using the textural triangle in accordance to the United States Department of Agriculture method (USDA) (Brown, 2003), then from the correspondence table of Stone and Hilborn (2001), the corresponding K values were deduced for each soil texture (Jemai et al., 2021).

2.2.3. The LS factor

The LS dimensionless shows the combined effects of topography parameters on the water erosion mechanism, the two important parameters which are L the length of the slope and S is the degree of inclination. An increase in these parameters leads to an increase in the LS factor producing higher surface runoff and greater erosion (Belasri & Lakhouili, 2016). Several formulas have been created to calculate the factor (Moore & Wilson, 1992). In the context of this study, the (Eq. 4), developed by Mitasova et al. (1996) and applied by several authors (Li & Shi, 2024; Saoud & Meddi, 2022), has been used:

$$LS = \left(\frac{FA \times A}{22.13} \right)^{0.4} \times \left(\frac{0.1745 \times \sin\theta}{0.0896} \right)^{1.4} \quad (4)$$

Where FA x A is the specific area (m^2/m), FA represents the flow accumulation, indicating the total upslope contributing area for a specific cell. A the cell size of the DEM (10 by 10 m) and θ is the slope (degree), With the incorporation of DEM into GIS, these parameters can be obtained to form the LS topographic factor.

2.2.4. The C factor

Cover factor C (dimensionless) is based on the density and height of ground surface vegetation cover (Wischmeier & Smith, 1978). It is the second most important factor after the topography factor controlling the risk of soil erosion (Van Der Knijff et al., 2000). The C Factor represents the effect of cultural practices and plant cover on reducing soil loss (Wang et al., 2002), where vegetation ensures the absorption of raindrops, slowing down runoff and infiltration. Generally, the values of the cover factor C vary from 0.001 for well-covered soils up to 1 as the maximum value for bare soils. Many methods have been developed to estimate the C factor using the NDVI (The Normalized Difference Vegetation Index) derived from satellite images (Ostovari et al., 2020). NDVI is frequently used to study the influence of land surface temperature (LST) on vegetation cover (Ullah et al., 2023; Sandholt et al., 2002). LST is also impacted by land use land cover (LULC) types through reflectance and surface roughness (Ullah et al., 2023; Li et al., 2017). The NDVI is calculated as a ratio between the spectral reflectance in red (R) and the spectral reflectance in near infrared (NIR) values (Eq. 5), obtained under GIS from the Sentinel 2 satellite image acquired in December of the year 2022 with a spatial resolution of 10 meters.

$$NDVI = \frac{NIR - RED}{NIR + RED} \tag{5}$$

The regression relation (Eq. 6) of Van Der Knijff et al. (2000) was applied for the calculation of the factor C:

$$C = e^{-\alpha \times \left(\frac{NDVI}{\beta - NDVI}\right)} \tag{6}$$

Whose parameters α, β determine the shape of the curve connecting the NDVI to the factor C. Van Der Knijff et al. (2000) proposes α the value 2 and β the value 1 in accordance with numerous works (Tashayo et al., 2020).

2.2.5. The P factor

The P factor (dimensionless) is the rate of soil loss (Renard et al., 1997) and takes into account human practices which preserve the soil against water erosion, for example the shape of contour lines, strip crops contour, earthworks and ridging (Wischmeier & Smith, 1978). The value of the P factor generally varies from 1 for bare soils on which no erosion control practices have been used and 0 in soils with low slope, managed and well protected (Ganasri & Ramesh, 2016). However, given the fact that there are no erosion control practices adopted throughout the study area, the number 1 was assigned to the factor P over all THNP regions.

3. Result and discussion

3.1. R factor results

The results of the rainfall erosivity index R, calculated from the measurements of the 10 rainfall stations bordering the THNP and then interpolated (Figure 3), show that the values vary from 75.78 (MJ.mm/ha.h.year) in the southern to 79.92 (MJ.mm/ha.h.year) in the Northern of THNP, with an average of 77.68 (MJ.mm/ha.h.year).

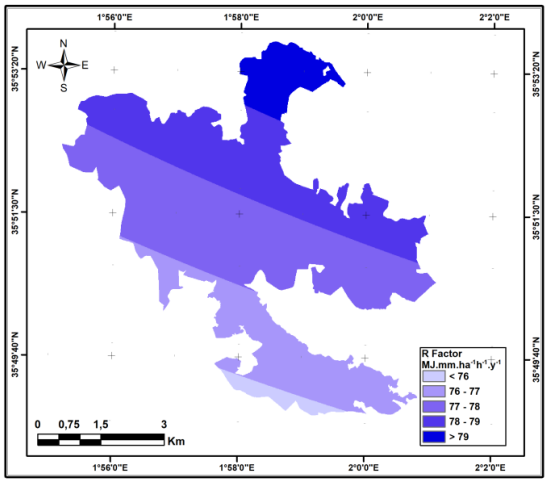

Figure 3. R factor map of the THNP

The rain erosivity index map makes it possible to delimit five classes of erosivity according to their aggressiveness coded from 1 to 5 (Table 2), in terms of areas, more than 77.50 % of the values of the THNP rainfall erosivity index R are greater than 77 (MJ.mm/ha.h.year), while the rest of the park shows values lower than 77 (MJ.mm/ha.h.year).

Table 2. The R factor classes in the THNP

ID	R factor	Area (ha)	Area (%)
1	< 76	99	2.90
2	76 – 77	660	19.50
3	77 – 78	1410	41.00
4	78 – 79	995	29.00
5	> 79	260	7.60

3.2. K factor results

The spatialization of the K factor shows that the values of erodibility in the THNP differ according to the type of soil (Figure 4). These values were derived from the Stone and Hilborn (2001) table by assigning to each soil texture the value of the factor K (Table 3).

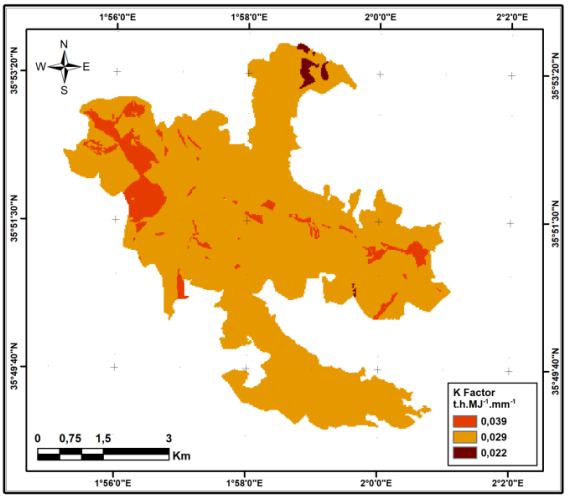

Figure 4. K factor map of the THNP

Table 3. Values of the K factor by soil type in the THNP

ID	Lithology	K factor (t.h/MJ.mm)	Area (ha)	Area (%)
1	Heavy clay	0.022	30.25	0.90
2	Clay	0.029	3126.79	91.30
3	Sandy clay	0.039	266.96	7.80

The results show that the soil texture is mostly clayey and the values of the K factor indicate that only 0.90 % of the THNP has a low erodibility of 0.022 (t.h./MJ.mm) for soils with a heavy clay texture, 91.30 % of the area of the study area has an average erodibility of 0.029 (t.h./MJ.mm) for the texture of the clay which is the most dominant and that the high values of the K factor represent 7.80 % of the soils of the THNP characterized by a sandy clay texture most vulnerable to erosion with a value of 0.039 (t.h./MJ.mm).

3.3. C factor results

The results of Factor C in the study site (Figure 5) are generated from the NDVI vegetation index which is a reliable and efficient tool (Ostovari et al., 2017). The analysis of the distribution map of five classes (Table 4), taken from the resulting map, shows that the values range between 0.2 and 0.8, with an average of 0.34., classes 0.2-0.4 dominate by a significant rate of vegetation cover 72 % of the area of the THNP. The heavily vegetated parts, generally covered with forest massifs, are assigned by the lowest values of C (<0.2) that covers 9.8 % of the THNP area, representing a better soil erosion protection, in contrast the highest values of the C factor (>0.8) which represents 0.7 % of the THNP area concern the parts with bare soils or low vegetation cover which are highly erodible soils. On the other hand, the parts whose factor C is between 0.2 and 0.8 are soils covered by moderately dense vegetation.

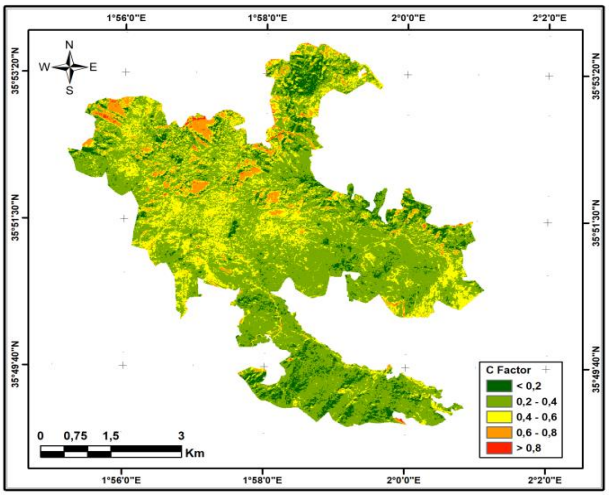

Figure 5. C factor map of the THNP

Table 4. The C factor classes in the THNP

ID	C factor	Area (ha)	Area (%)
1	< 0.2	337.35	9.8
2	0.2 - 0.4	2125.25	62.1
3	0.4 – 0.6	759.30	22.2
4	0.6 - 0.8	178.20	5.2
5	> 0.8	23.90	0.7

Water erosion depends on land use, a wooded soil slows down the kinetic energy of rain and intercepts part of the precipitation, leading to the reduction of soil erosion and the ecological restoration of the park. It is necessary to use anti-erosion techniques such as afforestation and intense reforestation which fix the soil and restore its stability.

3.4.LS factor results

The topographic factor LS changes based on the length of the slope (L) and the steepness of the incline (S). Therefore, the map obtained presents seven classes (Figure 6). LS values vary from 0 to 103.6 with an average of 2.70. The examination of the results shows that 35 % of the total area of the THNP (Table 5) representing minimum classes from 0 to 1, distributed over the study site, are generally located in the high altitude parts characterized by a low slope, which are not very sensitive to the erosion phenomenon, the greater part of 50 % of the area is occupied by the moderate classes between 1 and 5 %, the remaining 15 % scattered in the THNP correspond to the upper classes from 5 to 103.6, generally located in the high altitude parts with high slopes accelerating the runoff and, consequently, the water erosion process. This phenomenon, which depends on the nature of the soil, geology, and protection by plant cover, the implementation of hydraulic developments such as hedges and benches and terraces, proves effective in mitigating excessive runoff and protect the soil against this scourge.

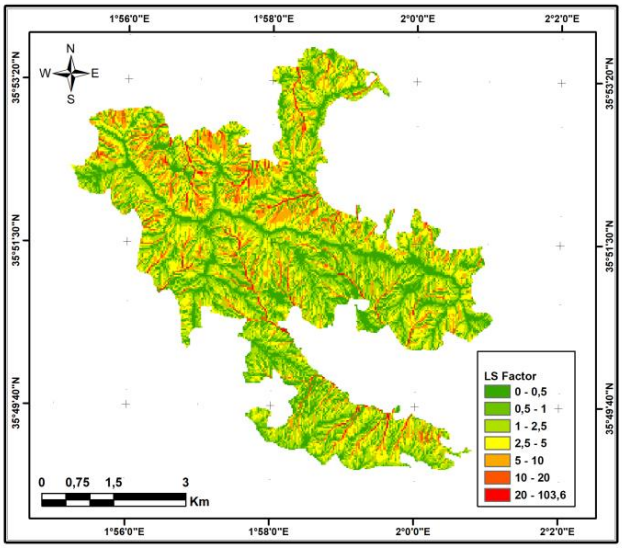

Figure 6. LS factor map of the THNP

Table 5. The LS factor classes in the THNP

ID	LS factor	Area (ha)	Area (%)
1	0 - 0.5	779.30	22.76
2	0.5 - 1	420.70	12.29
3	1- 2.5	1024.30	29.92
4	2.5 - 5	690.40	20.16
5	5 - 10	350.90	10.25
6	10 - 20	121.10	3.54
7	20 - 103.6	37.30	1.09

3.4. P factor results

Throughout the THNP the P factor was set at the value 1, since the anti-erosion measures cover modest areas not observed on the Sentinel 2 satellite images.

3.5. Annual soil loss results

The combination of the resulting maps of the different factors (R, K, C and LS) that make up the USLE equation of Wischmeier and Smith (1978) helped to establish the map of factor A, which indicates the average annual soil loss values in (t/ha.year) (Figure 7). The spatial distribution of soil losses shows that the THNP presents variability in terms of soil erosion according to the influence of the various factors controlling the phenomenon. For improved spatial visualization, the soil loss map has been divided into five classes based on their levels of aggressiveness (Table 6). Analysis of the results indicates soil losses varying between 0.02 and 55.10 (t/ha.year), with an average value 6.64 (t/ha.year) (Table 7).

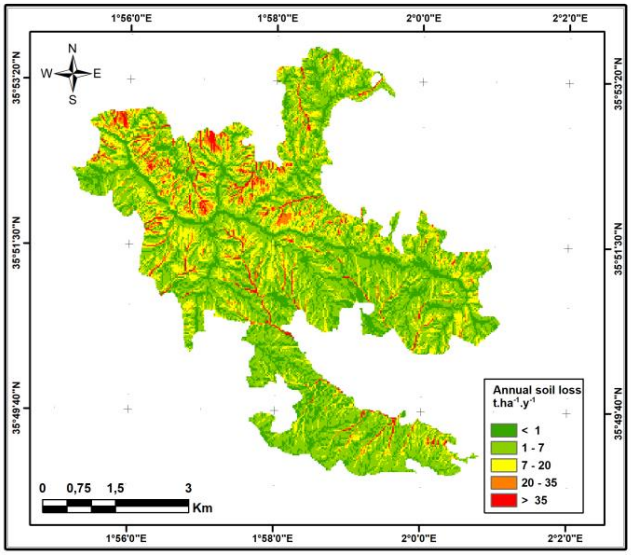

Figure 7. Annual Soil loss map of the THNP

Table 6. The Annul soil loss classes in the in the THNP

Annul soil loss (t/ha.year)	Erosion classes	Area (ha)	Area (%)
< 1	Very low	811	23.70
1 - 7	Low	1529	44.65
7 -20	Moderate	778	22.72
20 - 35	High	151	4.41
> 35	Very high	155	4.52

Table 7. Descriptive statistics of USLE results

Statistics	R (MJ.mm/ha.h.year)	K (t.h/MJ.mm)	LS (-)	C (-)	A (t/ha.year)
Maximum	79.92	0.0395	103.559	0.9854	55.01
Minimum	75.78	0.0223	0	0.0310	0.02
Mean	77.67	0.0297	2.70	0.3405	6.64

A percentage erosion class of 23.70, distributed over the total area of the study area, whose soil loss values are between 0.02 and 1 (t/ha.year), represents a very low concentration, which coincides with the low LS values associated with a more or less dense forest vegetation cover, These soils are noticeably very weak to erosion, the map analysis indicates a predominance of soils with low loss rates, which varies between 1 and 7 (t/ha.year) distributed over 44.65 % of the entire study area, the class varying between 7 and 20 represents an average erosion of around 22.72 %, these two classes are characterized by moderate LS values and forest vegetation cover, while the classes respectively with strong erosion between 20 and 35 and very strong erosion between 35 and 55.10 cover the northern part of 8.93 % of the surface of the THNP, where precipitation erosivity values (R>79) coincide with bare soils or soils with low vegetation cover (C>0.6), characterized by a very rugged relief with LS values (> 5), these sandy clay-textured soils with high K values are sensitive to the phenomenon of water erosion (Saoud & Meddi 2022; Ogawa et al., 2021).

Several studies on water erosion, carried out in mountainous ecosystems in different regions of the world, with similar environmental and climatic characteristics showing harmonic results with those obtained in the THNP. The work of Peng et al. (2022) carried out in the Qilian Mountain National Park located in North West China resulted in soil losses between 4.89 to 23.64 (t/ha.year), similar values were obtained by Shrestha (1997) in the mid-mountain region in the Nepalese Himalayas with a rate of 1 to 56 (t/ha.year). In the Alpine North-West of Italy, Stanchi et al. (2015) estimated rates from 0 to 26 (t/ha.year). In Ethiopia, Tamene et al. (2017) estimated this rate of 0.4 to 88 (t/ha.year), Wagari and Tamiru (2021) found the average annual of soil loss from 0.0 to 76.5 (t/ha.year) in Abay River Basin. The work of El Jazouli et al. (2017) in Ikkour watershed in the Middle Atlas of Morocco obtained annual soil loss varying between 0.0 to 70.66 (t/ha.year). In Oued El Hamma catchment south-eastern of Tunisia, Jemai et al. (2021) found a mean soil loss rate approximately 0.2 (t/ha.year) and estimated rates of 0.0 to17 (t/ha.year) in Matmata mountainous regions. In Algeria, similar results were found spread across the entire territory. In the North-East, Medjani et al. (2023) obtained rates which vary between 1 to more than 10 (t/ha.year) at the Tunisian border, and those of Bouhadeb et al. (2018) in the Bou Namoussa slope in El-Taref, showed rates varying between values less than 2 to greater than 20 (t/ha.year), in the Algerian Center, Koussa and Bouziane (2018) obtained loss values varying between 1.5 and 23 (t/ha.year) in the regions of Hassi bahbeh and Masàad. Finally, and in southwest Algeria, Melalih and Mazour (2021) reported values between 0 and 50 (t/ha.year) in the watershed of the Ksour mountains in Ain Sefra.

This study made it possible to estimate soil erosion rates in the THNP ; some of these particles will be transported to the watercourse and then their deposits, which is a factor in the siltation of dams of Beni Chaib and that of Meghila located downstream of the Park. The results provide information that can be a decision-making tool in developing strategies to mitigate the effects of land degradation. These results can be applied to the northern part of the THNP, a very vulnerable area, to minimize the impact of this phenomenon. Improving soil stability, reducing erosion and promoting biodiversity through the planting of native trees can contribute to the restoration of degraded ecosystems. In addition, the implementation of phytotechnical and hydraulic developments such as hedges and benches and terraces, proves effective in mitigating excessive runoff and protecting the soil against this scourge.

4. Conclusions

This study is carried out with the aim of estimating soil losses causing the risk of degradation of a mountainous ecosystem located at the THNP in northwestern Algeria using the USLE equation by integrationg GIS and RS techniques to develop a water erosion risk map. The THNP presents two main exhibitions; the North is more vulnerable to water erosion, characterized by a very high

degree of rain erosivity, compared to the South where there is a mountain massif constituting a barrier against rainfall between the two slopes north and south. The South-West and East parts are moderately vulnerable compared to the others. These results provide information on the spatial distribution of the phenomenon allowing the identification of areas at risk of degradation of the Park, priorities for intervention through soil conservation measures to curb this scourge and ensure sustainable management of these soils. The results from this model showed spatial variability in soil losses in the THNP. They showed that the classes with very low (<1) (t/ha.year) and low (1-7) (t/ha.year) erosion risk occupy respectively 23.70 % and 44.65 % of the THNP and represent almost all of the study area. 22.72 % of the soils of the study site are classified as moderate at risk of erosion (7-20) (t/ha.year), while the high erosion risk class (20 – 35) (t/ha.year) represents 4.41 %, the class characterized by a very high erosion risk (>35) (t/ha.year) covers 4.52 % of the THNP soils. According to the resulting soil loss map, the class with a very high risk of erosion is observed in the northern part of the THNP due to the very rugged relief characterized by soils bare or with low vegetation cover, however the classes with very low and low erosion risk are distributed over the study area in areas with low slopes associated with a more or less dense forest vegetation cover. Application of the USLE model has proven its effectiveness as a simple and practical tool for soil erosion risk assessment when integrated with GIS and RS techniques, at the same time; it provides useful information to decision makers to make informed decisions to control the risk of erosion. Managing soil erosion and protecting the THNP are crucial aspects to preserve its ecological integrity and the sustainability of its ecosystems. This study allowed us to carry out an in-depth assessment of the erosion risks in this park and to classify the areas according to their vulnerabilities. In perspective, this work will be applied with other comparative methods, taking into account the dynamics of land use, it would be possible to consider spatio-temporal monitoring of the factors C, K, R and LS to refine the estimate land loss.

Acknowledgement

The authors thank the THNP for making the data available. The authors wish to express their gratitude to the anonymous reviewers for their critical reviewing of the manuscript.

Author's declaration and contribution

The authors declare the absence of conflict of interest. Author Contribution FS Conception of the original idea, use of software, wording, visualization and supervision. BB, LG, AH, MNB, AE and AH data curation, formal analysis, wording, original draft, visualization, review and editing. All authors read and approved the final version of the manuscript.

References

Belasri, A., & Lakhouili, A. (2016). Estimation of soil erosion risk using the universal soil loss equation (USLE) and geo-information technology in Oued El Makhazine Watershed, Morocco. *Journal of Geographic Information System*, *8*(01), 98. CrossRef

Belay, T., Melese, T., & Senamaw, A. (2022). Impacts of land use and land cover change on ecosystem service values in the Afroalpine area of Guna Mountain, Northwest Ethiopia. *Heliyon*, *8*(12). CrossRef

Benchetrit, M. (1972). L'érosion actuelle et ses conséquences sur l'aménagement en Algérie. [Currenterosion and itsconsequences on development in Algeria]. *Revue Géographique des Pays Méditerranéens*, *tome 15*(4-1973), 115-116. Direct Link.

Bensekhria, A., & Bouhata, R. (2022). Assessment and mapping soil water erosion using RUSLE approach and GIS tools: case of ouedel-Hai watershed, Aurès West, Northeastern of Algeria. *ISPRS International Journal of Geo-Information*, *11*(2), 84. CrossRef

Benzater, B., Elouissi, A., Benaricha, B., & Habi, M. (2019). Spatio-temporal trends in daily maximum rainfall in northwestern Algeria (Macta watershed case, Algeria). *Arabian Journal of Geosciences*, *12*, 1-18. CrossRef

Bouguerra, H., Bouanani, A., Khanchoul, K., Derdous, O., & Tachi, S. E. (2017). Mapping erosion prone areas in the Bouhamdane watershed (Algeria) using the Revised Universal Soil Loss Equation through GIS. *Journal of Water and Land Development*, *32*(1), 13. Direct Link.

Bouhadeb, C. E., Menani, M. R., Bouguerra, H., & Derdous, O. (2018). Assessing soil lossusing GIS based RUSLE methodology. Case of the Bou Namoussa watershed–North-East of Algeria. *Journalof Water and Land Development*, *36*(1), 27-35. CrossRef

Bou-Imajjane, L., & Belfoul, M.A. (2020). Soil loss assessment in Western High Atlas of Morocco: Beni Mohand watershed study case. *Hindawi, Applied and Environmental Soil Science*, *2020*(1), 1-15. CrossRef

Brown, R. B. (2003) *Soil texture. University of Florida, IFAS Extension*. Direct Link.

Djoukbala, O., Hasbaia, M., Benselama, O., & Mazour, M. (2019). Comparison of the erosion prediction models from USLE, MUSLE and RUSLE in a Mediterranean watershed, case of Wadi Gazouana (NW of Algeria). *Modelling Earth Systems and Environment*, *5*(2), 725-743. CrossRef

El Jazouli, A., Barakat, A., Ghafiri, A., El Moutaki, S., Ettaqy, A., & Khellouk, R. (2017). Soil erosion modeled with USLE, GIS, and remote sensing: a case study of Ikkour watershed in Middle Atlas (Morocco). *Geoscience Letters*, *4*(1), 25 CrossRef

Ferreira, C. S., Seifollahi-Aghmiuni, S., Destouni, G., Ghajarnia, N., & Kalantari, Z. (2022). Soil degradation in the European Mediterranean region: Processes, status and consequences. *Science of the Total Environment*, *805*, 150106. CrossRef

Ganasri, B. P., & Ramesh, H. (2016). Assessment of soil erosion by RUSLE model using remote sensing and GIS-A case study of Nethravathi Basin. Geoscience *Frontiers*, *7*(6), 953-961. CrossRef

Girmay, G., Moges, A., & Muluneh, A. (2020). Estimation of soil loss rate using the USLE model forAgewmariayam Watershed, northern Ethiopia. *Agriculture & Food Security*, *9*, 1-12. CrossRef

Hachemaoui, A., Elouissi, A., Benzater, B., & Fellah, S. (2022). Assessment of the hydrological impact of land use/cover changes in a semi-arid basin using the SWAT model (case of the Oued Saïda basin in western Algeria). *Modeling Earth Systems and Environment*, *8*(4), 5611-5624. CrossRef

Hassan, H. E. H., Charbel, L., & Touchart, L. (2018). Modélisation de l'érosion hydrique à l'échelle du bassin versant du Mhaydssé. Békaa-Liban [Modeling of water erosion at the scale of the Mhaydssé watershed. Bekaa-Lebanon]. *VertigO-la Revue Electronique en Sciences de l'Environnement*, *18*(1). CrossRef

Hategekimana, Y., Allam, M., Meng, Q., Nie, Y., & Mohamed, E. (2020). Quantification of soil losses alongthecoastal protected areas in Kenya. *Land*, *9*(5),137. CrossRef

Jemai, S., Kallel, A., Agoubi, B., & Abida, H. (2021). Soil erosion estimation in arid area by USLE model applying GIS and RS: Case of Oued El Hamma catchment, south-eastern Tunisia. *Journal of The Indian Society of Remote Sensing, 49*(6), 1293-1305. CrossRef

Khaoula, K., & Sihem, J. (2021). *Évaluation de l'érosion hydrique dans des bassins versants de la zone semi-aride tunisienne avec les modèles RUSLE et MUSLE couplés à un Système d'Information Géographique* [Assessment of water erosion in watersheds in the Tunisiansemi-arid zone with the RUSLE and MUSLE modelscoupledwith a Geographic Information System]. *Cahiers Agricultures*, *30*,7. CrossRef

Kolli, M. K., Opp, C., & Groll, M. (2021). Estimation of soil erosion and sediment yield concentration across the Kolleru Lake catchment using GIS. *Environmental Earth Sciences*, *80*(4), 161. CrossRef

Koussa, M., & Bouziane, M. (2018). *Apport du SIG a la cartographie des zones à risqued'érosionhydrique dans la région de Djelfa, Algérie* [Contribution of GIS to the mapping of areas at risk of water erosion in the region of Djelfa, Algeria]. *Lebanese Science Journal*, *19*(1), 31-46. CrossRef

Koussa, M., & Bouziane, M.T. (2019). Estimation des paramètres de l'érosion hydrique par Approche SIG/USLE: cas du bassin versant de l'Oued Arab (région de Khenchela, Nord-Est de l'Algérie) [Estimation of water erosion parameters by GIS/USLE approach: Case of the Oued Arab watershed (Khenchela region, North-East Algeria)]. *Agriculture and Forestry Journal*, *3*(1), 36-45. CrossRef

Lamine, T. M., M'hamed, M., Azouzi Blel, P., Mohamed, Z., & Benchabane, H. (2016) Etude Eco-Dendrométrique Du Dépérissement Du Cèdre De l'Atlas Dans Le Parc National De Theniet El Had "Algérie" [Eco-Dendrometric Study of Atlas Cedar Dieback in Theniet El Had National Park "Algeria"]. *European Scientifique Journal*, *12*(29), 112-123. CrossRef

Li, H., & Shi, D. (2024). Spatio-temporal variation in soil erosion on sloping farmland based on the integrated valuation of ecosystem services and trade-offs model: A case study of Chongqing, southwest China. *Catena*, *236*, 107693. CrossRef

Li, W., Cao, Q., Lang, K., & Wu, J. (2017). Linking potential heat source and sink to urban heat island: Heterogeneous effects of landscape pattern on land surface temperature. *Science of the Total Environment*, *586*, 457-465. CrossRef

Mahleb, A., Hadji, R., Zahri, F., Boudjellal, R., Chibani, A., & Hamed, Y. (2022). *Water-borne erosion estimation using the Revised Universal Soil Loss Equation (RUSLE) model over a semiarid watershed: Case study of Meskiana Catchment, Algerian-Tunisian Border*. *Geotechnical and Geological Engineering*, *40*(8), 4217-4230. CrossRef

Mairif, M., Bendifallah, L., & Doumandji, S. (2023). *Diversity of Odonates (Odonata, Anisoptera & Zygoptera) in the Theniet El Had National Park-North West of Algeria. Journal of Insect Biodiversity and Systematics*, *9*(1), 155-182. CrossRef

Mandal, A., Das, A., Das, M., & Pereira, P. (2023). A quantitative review of ecosystem services research in Himalayan mountainous region. *Environmental Challenges*, *100792*. CrossRef

Markose, V. J., & Jayappa, K. S. (2016). Soil loss estimation and prioritization of sub-watersheds of Kali River basin, Karnataka, India, using RUSLE and GIS. *Environmental Monitoring and Assessment*, *188*, 1-16. CrossRef

Meddi, M., Toumi, S., & Assani, A. A. (2016). Spatial and temporal variability of the rainfall erosivity factor in Northern Algeria. *Arabian Journal of Geosciences*, *9*, 1-13. CrossRef

Medjani, F., Derradji, T., Zahi, F., Djidel, M., Labar, S., & Bouchagoura, L. (2023). Assessment of soil erosion by Universal Soil Loss Equation model based on Geographic Information System data: A case study of the Mafragh watershed, north-eastern Algeria. *Scientific African*, *21*, e01782. CrossRef

Melalih, A., & Mazour, M. (2021). Using RUSLE and GIS for the soil loss assessment in arid regions: The case of the Ain Sefra catchment in the Ksour Mountains, *Algeria. Journal of Water and Land Development*, *48*, 205-214. Direct Link.

Milazzo, F., Fernández, P., Peña, A., & Vanwalleghem, T. (2022). The resilience of soil erosion rates under historical land use change in agroecosystems of Southern Spain. *Science of The Total Environment*, *822*, 153672. CrossRef

Mitasova, H., Hofierka, J., Zlocha, M., & Iverson, L. R. (1996). Modelling topographic potential for erosion and deposition using GIS. *International Journal of Geographical Information Systems*, *10*(5), 629-641. CrossRef

Moore, I. D., & Wilson, J. P. (1992). Length-slope factors for the Revised Universal Soil Loss Equation: Simplified method of estimation. *Journal of Soil and Water Conservation*, *47*(5), 423-428. Direct Link.

Nagdeve, M., Paul, P. K., Zhang, Y., & Singh, R. (2021). Continuous Contour Trench (CCT): Understandings of hydrological processes after standardisation of dimensions and development of a user-friendly software. *Soil and Tillage Research*, *205*, 104792. CrossRef

Ogawa, R., Hirata, M., Gebremedhin, B. G., Uchida, S., Sakai, T., Koda, K., & Takenaka, K. (2021). Spatial modeling of soil erosion and identification of high-risk spots with the GIS-RUSLE model for the Adi Zaboy watershed, eastern Tigray region, Ethiopia. *Journal of Arid Land Studies*, *31*(1), 1-14. CrossRef

Ostovari, Y., Ghorbani-Dashtaki, S., Bahrami, H. A., Naderi, M., & Dematte, J. A. M. (2017). Soil loss estimation using RUSLE model, GIS and remote sensing techniques: A case study from the Dembecha Watershed, Northwestern Ethiopia. *Geoderma Regional*, *11*, 28-36. CrossRef

Ostovari, Y., Moosavi, A. A., & Pourghasemi, H. R. (2020). Soil loss tolerance in calcareous soils of a semiarid region: evaluation, prediction, and influential parameters. *Land Degradation & Development*, *31*(15), 2156-2167. CrossRef

Panagos, P., Matthews, F., Patault, E., De Michele, C., Quaranta, E., Bezak, N., ... & Borrelli, P. (2024). Understanding the cost of soil erosion: An assessment of the sediment removal costs from the reservoirs of the European Union. *Journal of Cleaner Production*, *434*, 140183. CrossRef

Panagos, P., Standardi, G., Borrelli, P., Lugato, E., Montanarella, L., & Bosello, F. (2018). Cost of agricultural productivity loss due to soil erosion in the European Union: From direct cost evaluation approaches to the use of macroeconomic models. *Land Degradation & Development*, *29*(3), 471-484. CrossRef

Peng, Q., Wang, R., Jiang, Y., Zhang, W., Liu, C., & Zhou, L. (2022). Soil erosion in Qilian mountain national park: dynamics and driving mechanisms. Journal of Hydrology: *Regional Studies*, *42*, 101144. CrossRef

Rango, A., & Arnoldus, H. M. J. (1987). Aménagement des bassins versants [Watershed development]. *Cahiers Techniques de la FAO*, *36*, 1-11. Direct Link.

Rellini, I., Scopesi, C., Olivari, S., Firpo, M., & Maerker, M. (2019). Assessment of soil erosion risk in a typical Mediterranean environment using a high-resolution RUSLE approach (Portofino promontory, NW-Italy). *Journal of Maps*, *15* (2), 356-362. CrossRef

Renard, K. G., Foster G. R., Weesies G. A., McCool D. K., & Yoder D. C. (1997). Predicting soil erosion by water: a guide to conservation planning with the Revised Universal Soil Loss Equation (RUSLE). *US Department of Agriculture, Agricultural Research Service.* Direct Link.

Sahnoun, F., Abderrahmane, H., Kaddour, M., Abdelkader, K., Mohamed, B., & Castro, T. A. H. D. (2021). Application of SEBAL and T s/VI trapezoid models for estimating actual evapotranspiration in the Algerian semi-arid environment to improve agricultural water management. *Revista Brasileira de Meteorologia*, *36*, 219-236. CrossRef

Sandholt, I., Rasmussen, K., & Andersen, J. (2002). A simple interpretation of the surface temperature/vegetation index space for assessment of surface moisture status. *Remote Sensing of Environment*, *79*(2-3), 213-224. CrossRef

Saoud, M., & Meddi, M. (2022). Mapping of erosion using USLE, GIS and remote sensing in Wadi El Hachem Watershed (Northern Algeria): Case study. *Journal of the Indian Society of Remote Sensing*, *50*(3), 569-581. CrossRef

Sarmoum, M., Navarro-Cerrillo, R. M., Guibal, F., & Abdoun, F. (2018). *Structure, tree growth and dynamics of Cedrusatlantica Manetti Forests in Theniet El Had National Park (NW Algeria). Open Journal of Ecology*, *8*(8), 432-446. CrossRef

Sheikh, A. H., Palria, S., & Alam, A. (2011). Integration of GIS and universal soil loss equation (USLE) for soil loss estimation in a Himalayan watershed. *Recent Research in Science and Technology*, *3*(3) Direct Link.

Shrestha, D. P. (1997). Assessment of soil erosion in the Nepalese Himalaya: A case study in LikhuKhola Valley, Middle Mountain Region. *Land Husbandry*, *2*(1), 59-80. Direct Link.

Sonia, G., Hamdi, K., Abir, M., & Mohamed, K. (2022). The comparison between the Universal Soil Loss Equation (USLE) and the HEUSCH model for the assessment and mapping of water erosion of the Sidi Saad dam watershed in Tunisia. *Arabian Journal of Geosciences*, *15*(6), 466. CrossRef

Stanchi, S., Falsone, G., & Bonifacio, E. (2015). Soil aggregation, erodibility, and erosion rates in mountain soils (NW Alps, Italy). *Solid Earth*, *6*(2), 403-414. CrossRef

Stone, R. P., & Hilborn, D. (2001*). Universal soil loss equation, USLE. Sejong City, China*. Ministry of Agriculture, Food & Rural Affairs, Agriculture & Rural. CrossRef

Tamene, L., Adimassu, Z., Ellison, J., Yaekob, T., Woldearegay, K., Mekonnen, K., Thorne,P., & Le, Q. B. (2017). Mapping soil erosion hotspots and assessing the potential impacts of land management practices in the highlands of Ethiopia. G*eomorphology*, *292*, 153-163. CrossRef

Tashayo, B., Honarbakhsh, A., Akbari, M., & Ostovari, Y. (2020). Digital mapping of Philip model parameters for prediction of water infiltration at the watershed scale in a semi-arid region of Iran. *GeodermaRegional*, *22*, e00301. CrossRef

Toumi, S., Meddi, M., Mahé, G., & Brou, Y. T. (2013). Cartographie de l'érosion dans le bassin versant de l'Oued Mina en Algérie par télédétection et SIG [Mapping erosion in the Oued Mina watershed in Algeria using remote sensing and GIS]. *Hydrological Sciences Journal*, *58*(7), 1542-1558. CrossRef

Ullah, W., Ahmad, K., Ullah, S., Tahir, A. A., Javed, M. F., Nazir, A., ... & Mohamed, A. (2023). Analysis of the relationship among land surface temperature (LST), land use land cover (LULC), and normalized difference vegetation index (NDVI) with topographic elements in the lower Himalayan region. *Heliyon*, *9*(2). CrossRef

Van der Knijff, J. M., Jones, R. J. A., & Montanarella, L. (2000). Soil erosion risk assessment in Europe, EUR 19044 EN. *Office for Official Publications of the European Communities, Luxembourg*, 34. Direct Link.

Vrieling, A. (2006). Satellite remote sensing for water erosion assessment: A review. *Catena*, *65*(1), 2-18. CrossRef

Wagari, M., & Tamiru, H. (2021). RUSLE model based annual soil loss quantification for soil erosion protection: A case of Fincha Catchment, Ethiopia. Air, *Soil and Water Research*, *14*, CrossRef

Wang, G., Wente, S., Gertner, G. Z., & Anderson, A. (2002). Improvement in mapping vegetation cover factor for the universal soil loss equation by geostatistical methods with Landsat Thematic Mapper images. *International Journal of Remote Sensing*, *23*(18), 3649-3667. CrossRef

Wischmeier, W. H., & Smith, D. D. (1978). Predicting rainfall erosion losses: a guide to conservation planning (No. 537). *Department of Agriculture, Science and Education Administration. Direct Link.*

Xu, Z., Pan, B., Han, M., Zhu, J., & Tian, L. (2019). Spatial–temporal distribution of rainfall erosivity, erosivity density and correlation with El Niño–Southern Oscillation in the Huaihe River Basin, China. *Ecological Informatics*, *52*, 14-25. CrossRef

Yesuph, A. Y., & Dagnew, A. B. (2019). Soil erosion mapping and severity analysis based on RUSLE model and local perception in the Beshillo Catchment of the Blue Nile Basin, Ethiopia. *Environmental Systems Research*, *8*(1), 1-21. CrossRef